Cell Death & Differentiation (2019) 26:1107–1123
https://doi.org/10.1038/s41418-018-0187-3

Cell Death & Differentiation

ARTICLE

Multipoint targeting of TGF-β/Wnt transactivation circuit with microRNA 384-5p for cardiac fibrosis

Hyang-Hee Seo[1] · Seahyoung Lee[2] · Chang Youn Lee[3] · Jiyun Lee[1] · Sunhye Shin[3] · Byeong-Wook Song[4] · Il-Kwon Kim[2] · Jung-Won Choi[5] · Soyeon Lim[2] · Sang Woo Kim[2] · Ki-Chul Hwang[2]

Received: 15 January 2018 / Revised: 17 July 2018 / Accepted: 30 July 2018 / Published online: 11 September 2018

Abstract

Cardiac fibrosis is a common precursor to ventricular dysfunction and eventual heart failure, and cardiac fibrosis begins with cardiac fibroblast activation. Here we have demonstrated that the TGF-β signaling pathway and Wnt signaling pathway formed a transactivation circuit during cardiac fibroblast activation and that miR-384-5p is a key regulator of the transactivation circuit. The results of in vitro study indicated that TGF-β activated an auto-positive feedback loop by increasing Wnt production in cardiac fibroblasts, and Wnt neutralizing antibodies disrupted the feedback loop. Also, we demonstrated that miR-384-5p simultaneously targeted the key receptors of the TGF-β/Wnt transactivation circuit and significantly attenuated both TGF-β-induced cardiac fibroblast activation and ischemia-reperfusion-induced cardiac fibrosis. In addition, small molecule that prevented pro-fibrogenic stimulus-induced downregulation of endogenous miR-384-5p significantly suppressed cardiac fibroblast activation and cardiac fibrosis. In conclusion, modulating a key endogenous miRNA targeting multiple components of the TGF-β/Wnt transactivation circuit can be an effective means to control cardiac fibrosis and has great therapeutic potential.

Introduction

Although cardiac fibrosis initially occurs as a compensatory response to maintain the structural and functional integrity of the damaged heart, when it is severe and prolonged, ventricular dysfunction and, ultimately, heart failure can result [1, 2]. Activation of fibroblasts or myofibroblast (myoFB) formation by various cytokines constitutes an early event in cardiac fibrosis. For example, during the first 0-4 days after cardiac injury, called the inflammatory phase, massive death of cardiomyocytes occurs and the expressions of cytokines such as transforming growth factor-beta (TGF-β) increase, causing an inflammatory response. For the next 3–4 days, called the reparative phase, cytokines activate cardiac fibroblasts (CFs), which triggers the deposition of fibrogenic extracellular matrix [3]. In adult mammals, the fibrotic scar is permanent and further promotes reactive fibrosis, which increases myocardial stiffness and reduces compliance [2]. Therefore, prevention of CF activation can be an effective means to control cardiac fibrosis.

Both TGF-β [4–6] and Wnt signaling pathways [7] significantly contribute to cardiac fibrosis, and a possible interaction between these two pro-fibrogenic pathways has been suggested. Previous studies have reported that TGF-β-induced

Edited by P. Salomoni

These authors contributed equally: Hyang-Hee Seo, Seahyoung Lee.

Electronic supplementary material The online version of this article (https://doi.org/10.1038/s41418-018-0187-3) contains supplementary material, which is available to authorized users.

✉ Ki-Chul Hwang
kchwang@cku.ac.kr

[1] Brain Korea 21 PLUS Project for Medical Science, Yonsei University, Seoul, Republic of Korea

[2] Institute for Bio-Medical Convergence, College of Medicine, Catholic Kwandong University, Gangneung, Republic of Korea

[3] Department of Integrated Omics for Biomedical Sciences, Yonsei University, Seoul, Republic of Korea

[4] EIT/LOFUS R&D Center, International St. Mary's Hospital, Incheon, Republic of Korea

[5] Department of Environmental Engineering, Catholic Kwandong University, Gangneung, Republic of Korea

skin fibrosis requires Wnt signaling activation [8] and that Wnt3a induces myoFB differentiation of mouse embryonic fibroblasts in a TGF-β and β-catenin-dependent manner [9]. Recently, it was demonstrated that TGF-β controls myoFB formation via Wnt secretion in autoimmune myocarditis [10]. These studies strongly imply the existence of a TGF-β/Wnt transactivation circuit in fibrosis. Therefore, a careful examination of the mechanisms that underlie such a pro-fibrogenic transactivation circuit may provide critical information for developing a therapeutic strategy to disrupt the circuit and subsequently prevent cardiac fibrosis and heart failure.

MicroRNAs (miRNAs) negatively regulate the expression of target genes at the post-transcriptional level [11]. Presumably, thousands of miRNAs regulate approximately 30% of all coding genes in humans, affecting virtually every aspect of biological processes [12–14]. Therefore, miRNAs may contribute to the initiation and maintenance of the TGF-β/Wnt transactivation circuit, if it exists. Furthermore, since a single miRNA can target multiple genes simultaneously [15], a key miRNA that affects both signaling pathways may exist. In this study, as a proof of concept, we examined the hypotheses that a key miRNA mediates the formation and maintenance of a TGF-β/Wnt transactivation circuit and that modulating the expression of the key miRNA will disrupt the circuit, preventing progression of cardiac fibrosis.

Result

Characterization of primary cultured CFs

To characterize the primary cultured CFs, a number of parameters, including activation marker expressions before and after TGF-β treatment were evaluated (Supplementary Fig. 1), and the results indicated that our in vitro model of TGF-β-mediated activation of CF worked properly.

TGF-β activates canonical Wnt signaling in CFs

The expressions of cytoplasmic beta-catenin (β-catenin) and phosphorylated glycogen synthase kinase 3 beta (p-GSK3β^{ser9}), which are representative markers of canonical Wnt signaling activation [16], were increased by TGF-β (Fig. 1a). TGF-β significantly increased the nuclear translocation of β-catenin, a hallmark of activated canonical Wnt signaling [16], indicating that TGF-β activated canonical Wnt signaling in CFs at the given concentration (Fig. 1b).

Effect of ischemia/reperfusion and TGF-β on the expression of Wnts and related receptors

Wnt signaling is initiated by combinatorial interactions between 19 different Wnt ligands [17] and 10 different frizzled receptors (Fzds) [18]. Previous studies have reported that Fzd1 and Fzd2 were upregulated in cardiac myoFBs [19], and inhibition of the interaction between Wnt3a/Wnt5a and their putative receptors, Fzd1/Fzd2, prevented heart failure after myocardial infarction [20]. In this study, the mRNA expressions of Fzd1, Fzd2, Wnt3a, and Wnt5a significantly increased in the ischemia/reperfusion (I/R)-injured heart (Supplementary Fig. 2). In TGF-β treated CFs, the mRNA expressions of Fzd1 and Fzd2 significantly increased at 12 h (Fig. 1c, left panel), and Wnt3a mRNA expression also significantly increased at 1 h and thereafter up to 12 h. However, TGF-β had no significant effect on Wnt5a mRNA expression (Fig. 1c, right panel). A previous study examined the effect of secreted Frizzeled-related protein 2 (sFRP2) on Wnt3a and Wnt5a expression in CFs reported similar observation that sFRP2 significantly increased the Wnt3a expression, while it decreased the Wnt5a expression [21], suggesting that the transcription of those Wnt ligands may utilize different mechanisms. We speculated that cells other than CFs may be responsible for the observed increase of Wnt5a in the I/R-injured heart, and co-immunostaining results of I/R-injured heart showed that the expressions of Wnt3a and ER-TR7, a fibroblast marker, were co-localized (Supplementary Fig. 3a), while Wnt5a expression was co-localized to that of CD68 expression (Supplementary Fig. 3b).

Wnt3a mediates TGF-β-induced activation of an auto-positive feedback via NF-kB in CFs

TGF-β induces the expression of Wnt proteins via TGF-β-activated kinase 1 (TAK1) pathway [10]. TGF-β-induced TAK1 activation can lead to the activation of nuclear factor kappa-light-chain-enhancer of activated B cells (NF-kB), JNK, or p38 [22]. In this study, TGF-β did not affect the expressions of phosphorylated JNK and p38, whereas the expression of phosphorylated TAK1 and p65, a marker of NF-kB activation [23], significantly increased (Supplementary Fig. 4a) by TGF-β. Caffeic acid phenethyl ester (CAPE), a potent inhibitor of NF-kB (Supplementary Fig. 4b) [24], significantly decreased the expression of both p-IKKα and Wnt3a (Fig. 1d), indicating that TGF-β-induced Wnt3a production was mediated by NF-kB. Furthermore, Wnt3a significantly increased the expression of both β-catenin and TGF-β (Supplementary Fig. 5a), and TGF-β significantly increased the mRNA expression of TGF-β itself in a time-dependent manner for up to 4 h (Supplementary Fig. 5b). These data suggested that TGF-β activated an auto-positive feedback loop mediated by Wnt3a. Wnt3a-neutralizing antibodies significantly attenuated the expressions of β-catenin and p-GSK3β^{ser9} and also significantly suppressed TGF-β and collagen type I expressions (Fig. 1e). Furthermore, both CAPE and FH535, a Wnt/β-catenin signaling inhibitor [25], significantly suppressed the production of TGF-β (Fig. 1f). These data

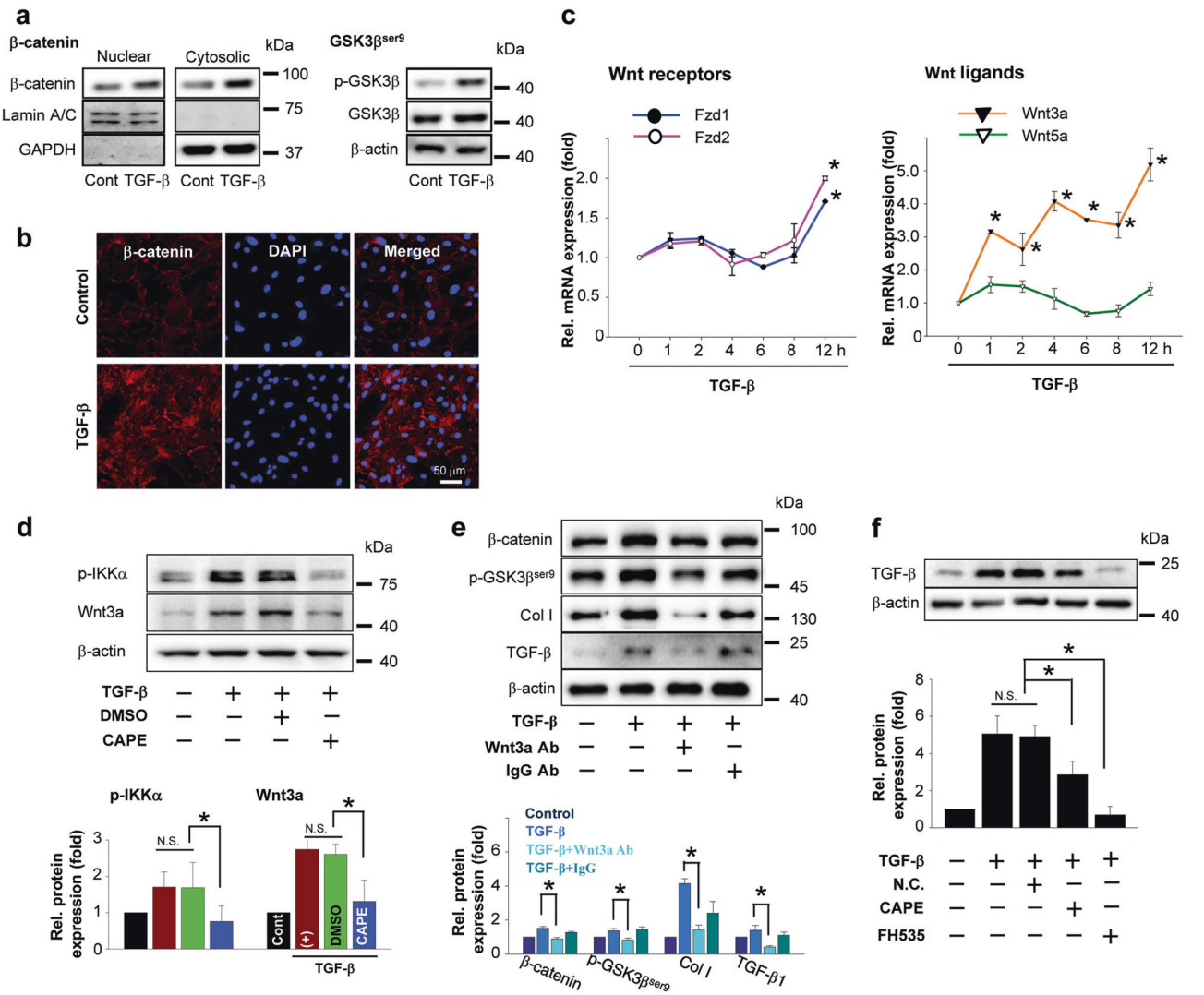

Fig. 1 Wnt3a links TGF-β signaling and Wnt signaling in TGF-β activated CFs. **a** Left panel: Serum-starved CFs were treated with 5 ng/ml TGF-β for 30 min, and cytosolic and nuclear expression of β-catenin was detected by western blotting. Lamin A/C and GAPDH were used as internal controls for the nuclear and cytosolic fraction, respectively. Right panel: the expression of p-GSK3β^{ser9} following TGF-β treatment was examined by western blotting. **b** Immunocytochemical staining of β-catenin. Nuclei were stained with DAPI. **c** The mRNA expression levels of Fzd1, Fzd2, Wnt3a, and Wnt5a in the TGF-β-treated primary CFs. The cells were treated with 5 ng/ml TGF-β for up to 12 h as indicated. Untreated CFs were used as a control. *$p < 0.05$ compared to the control. **d** The cells were treated with 5 ng/ml CAPE for 30 min and then further exposed to TGF-β (5 ng/ml) for 2 h. The expression levels of p-IKK and Wnt3a were examined by western blotting. Untreated CFs were used as a control. *$p < 0.05$. **e** The cells were treated with TGF-β (5 ng/ml) for 4 h with or without Wnt3a-neutralizing antibodies (15 μg/ml), and the expression levels of β-catenin, p-GSK3β^{ser9}, TGF-β, and collagen type I (Col I) were examined by western blotting. *$p < 0.05$ compared to the TGF-β-treated control. **f** The cells were treated with TGF-β (5 ng/ml) for 4 h in the presence of CAPE (5 μg/ml), an NF-kB inhibitor, and FH535 (15 μM), a Wnt/β-catenin signaling inhibitor, and the expression levels of TGF-β were examined by western blotting. *$p < 0.05$. Quantitative data were expressed as the mean ± S.E.M. of at least 3 independent experiments. N.S not significant, IKK Inhibitor of kappa B kinase

indicate that TGF-β induces production of Wnt3a, which in turn increases TGF-β production, establishing a transactivation circuit between TGF-β and Wnt signaling pathways in CFs.

MiR-384-5p targets multiple receptors of the TGF-β/Wnt transactivation circuit

A single miRNA can target multiple genes simultaneously. Therefore, a key miRNA that regulates the initiation and maintenance of the circuit affecting both signaling pathways may exist. To find such miRNA(s), a miRNA-target mRNA prediction database (www.targetscan.org) was utilized. Because ligands of TGF-β and Wnt signaling can be also produced by cardiac cells other than CFs, down-regulation of ligands in CFs may not be sufficient to disrupt the circuit in vivo. Thus, key receptors of the circuit were assumed as primary targets in the screening of miRNAs. Fzd1 and Fzd2 have been implicated in cardiac

fibrosis [19], and they were also increased in the present study (Fig. 1c and Supplementary Fig. 2). Tgfbr1 is one of the main receptors for TGF-β signaling [26], and Lrp5 and Lrp6 are well-known co-receptors for Wnt signaling [27]. Thus, these 5 receptors were chosen as possible primary targets. Among the miRNAs predicted to target each receptor (Supplementary Tab. 1), only 2 miRNAs (miR-141-3p and miR-384-5p) were predicted to target 4 out of 5 receptors, namely, Fzd1, Fzd2, Tgfbr1, and Lrp6 (Fig. 2a). As shown in Fig. 2b, compared to miR-141-3p, miR-384-5p significantly suppressed the expressions of predicted targets. To verify whether the decreased expression was directly mediated by miR-384-5p, luciferase assays were conducted (Fig. 2c). The luciferase activity was

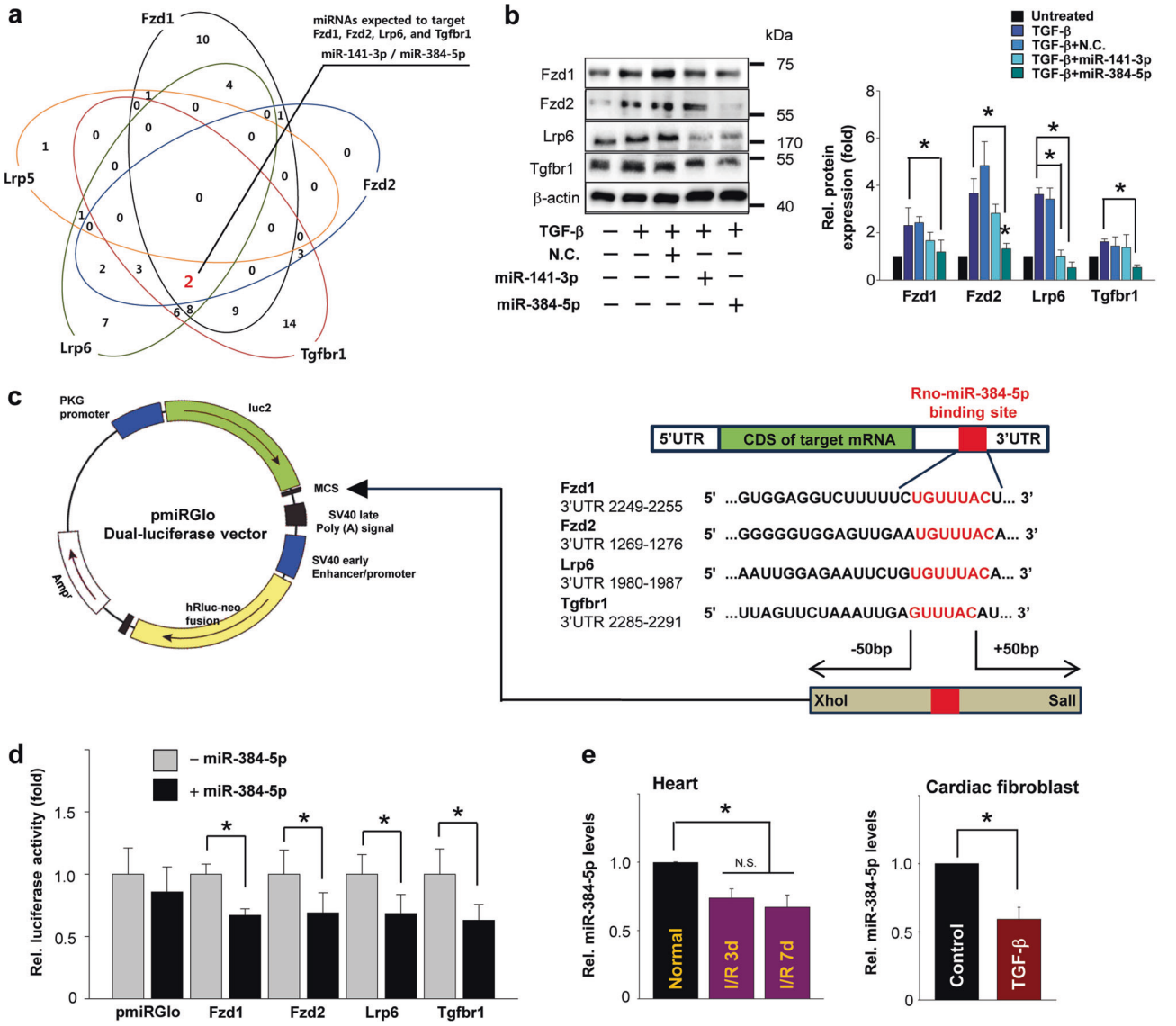

Fig. 2 MiR-384-5p targets multiple receptors of the TGF-β-Wnt transactivation circuit. **a** MicroRNAs predicted to target the 5 key receptors of the TGF-β and Wnt signaling pathways were analyzed to identify miRNAs targeting most of the receptors. The number in the Venn diagram indicates the number of miRNAs belonging to the corresponding intersection. **b** The cells were transfected with either 100 nM miR-141-3p or 100 nM miR-384-5p for 24 h. The expression levels of predicted targets (Fzd1, Fzd2, Tgfbr1, and Lrp6) were examined by western blotting. $*p < 0.05$. **c** Schematic presentation of luciferase vector construction. The miR-384-5p-binding site in the 3'UTR of Fzd1, Fzd2, Tgfbr1, and Lrp6 was cloned into the pmirGLO vector using Xho I and Sal I restriction enzymes. **d** Luciferase vectors containing the miR-384-5p-binding sites of each receptor were delivered to HeLa cells with or without co-delivery of miR-384-5p. Twenty-four hours after the transfection, luciferase activity was measured. $*p < 0$. **e** The expression levels of miR-384-5p in the I/R-injured heart and TGF-β-treated CFs were examined. Three and 7 days after the injury, the heart tissue was collected, and the expression of miR-384-5p was detected by real-time PCR. Normal heart tissue was used as a control. Primary CFs were treated with 5 ng/ml TGF-β for 24 h, and the expression of miR-384-5p was detected by real-time PCR, $*p < 0.05$. Quantitative data were expressed as the mean ± S.E.M. of at least 3 independent experiments. N.S not significant

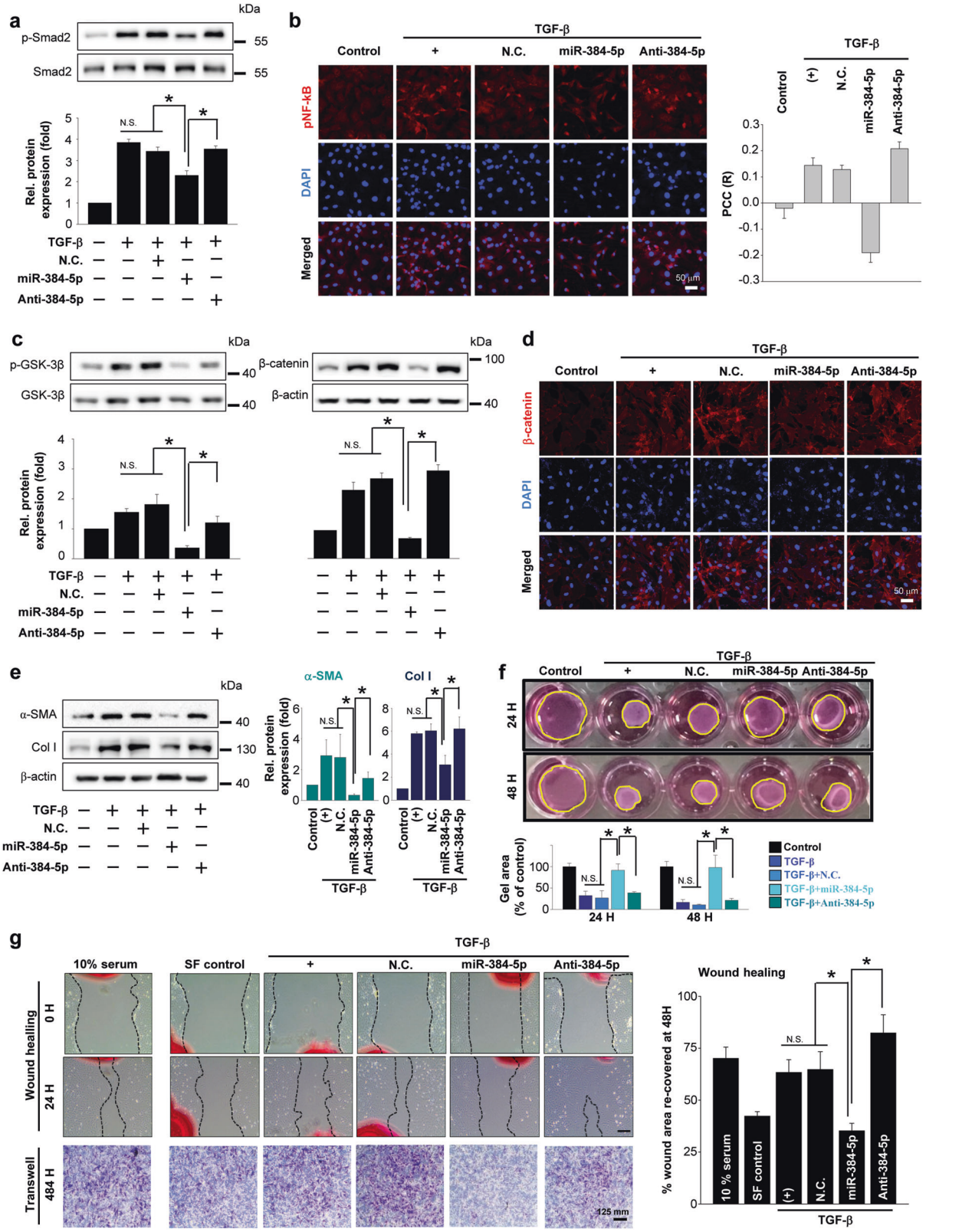

significantly decreased by miR-384-5p in all cases, indicating that those 4 receptors were direct targets of miR-384-5p (Fig. 2d).

Lastly, the expression of miR-384-5p in I/R-injured heart or in TGF-β-treated CFs was examined. As shown in Fig. 2e, the expression of miR-384-5p significantly

◀ **Fig. 3** MiR-384-5p attenuates TGF-β-induced CF activation. **a** The cells were transfected with 100 nM miR-384-5p or anti-miR-384-5p for 24 h and then treated with TGF-β for an additional 24 h. The expression levels of p-Smad was examined, $*p < 0.05$. **b** Nuclear translocation of pNF-kB was detected by using immunocytochemistry. Co-localization of pNF-kB and DAPI was expressed as the Pearson's correlation coefficient R (PCC). Nuclei were stained with DAPI. **c** The expression levels of signaling molecules in the Wnt/β-catenin pathway were examined. $*p < 0.05$. **d** The cells were transfected with either 100 nM miR-384-5p or 100 nM anti-miR-384-5p for 24 h and then exposed to 5 ng/ml TGF-β for an additional 24 h. The expression of β-catenin was visualized by immunocytochemistry. Nuclei were stained with DAPI. **e** The cells were transfected with 100 nM miR-384-5p for 24 h. The expression of α-SMA and collagen type I (Col I) was examined by western blotting. $*p < 0.05$. **f** CF-containing collagen gels were serum-starved for 12 h. After starvation, gels were stimulated with TGF-β (5 ng/ml) for 48 h and photographed at 24 h and 48 h. The sizes of the gels were measured and analyzed. $*p < 0.05$. **g** For the wound-healing analysis, the cells were transfected with 100 nM miR-384-5p for 24 h. The images of the wounds were obtained at 0 and 24 h. The area between the wound edges was measured and compared among the groups (right panel). $*p < 0.05$. Quantitative data were expressed as the mean ± S.E.M. of at least 3 independent experiments. For the migration analysis, the cells were seeded in the upper chambers of Transwells and transfected with either 100 nM miR-384-5p or 100 nM anti-miR-384-5p for 24 h. The cells were further treated with TGF-β for an additional 24 h. The migrated cells were stained with crystal violet. N.S not significant. NC negative control scrambled miRNA. SF serum free

decreased at 3 and 7 days after the I/R injury, and 24 h of TGF-β treatment also significantly decreased the expression of miR-384-5p in CFs. These data suggest that miR-384-5p is a key regulator of the circuit and downregulation of miR-384-5p during I/R-injury promotes CF activation and subsequent cardiac fibrosis by enhancing the expression of key receptors of the circuit.

MiR-384-5p attenuates the activation of TGF-β and Wnt signaling

The effects of miR-384-5p on TGF-β and Wnt signaling pathways were examined. As shown in Fig. 3a, miR-384-5p inhibited the activation of Smad pathway. Furthermore, miR-384-5p inhibited nuclear translocation of pNF-kB (Fig. 3b) and DNA binding of NF-kB p65 (Supplementary Fig. 6). MiR-384-5p decreased the phosphorylation of $GSK3\beta^{ser9}$ and β-catenin (Fig. 3c), and this indicated that miR-384-5p suppressed the TGF-β-induced activation of Wnt/β-catenin signaling in CFs. Moreover, miR-385-5p prominently attenuated the TGF-β-induced nuclear translocation of β-catenin (Fig. 3d).

MiR-384-5p inhibits CF activation

Exogenous miR-384-5p (100 nM, 24 h) significantly decreased the expression of both α-SMA (Supplementary Fig. 7) and collagen type I (Fig. 3e), suggesting attenuated CF activation. Collagen gel contraction analysis demonstrated that miR-384-5p significantly attenuated TGF-β-induced collagen contractility of CFs (Fig. 3f). The results of migration assays indicated that miR-384-5p suppressed migration of TGF-β-treated CFs (Fig. 3g).

MiR-384-5p attenuates cardiac fibrosis following I/R-injury

Exogenous miR-384-5p (10 μg/head) was delivered to the heart following I/R-injury. Up to 14 days after the injury, the level of miR-384-5p was well maintained (Fig. 4a). The expressions of Fzd-1, Fzd-2, Lrp6, and Tgfbr1 significantly decreased with miR-384-5p delivery (Fig. 4b). Most importantly, exogenous miR-384-5p significantly attenuated cardiac fibrosis (Fig. 4c) as evidenced by the significantly decreased fibrotic area (Fig. 4d) and well-maintained left ventricular (LV) wall thickness (Fig. 4e). Furthermore, I/R-induced decline of heart function evaluated by cardiac output (Fig. 4f), systemic volume (Fig. 4g), and ejection fraction (Fig. 4h) was significantly attenuated by exogenous miR-384-5p.

The liver, kidney, and spleen of animals were H & E stained to examine any significant adverse effect following miR-384-5p administration. The key structures of the organs examined (portal vein, Bowman's capsule, and white pulp for the liver, kidney, and spleen, respectively) were intact and no significant tissue damage was observed (Supplementary Fig. 8). These data indicated that exogenous miR-384-5p significantly suppressed cardiac fibrosis and improved heart function without any significant adverse effect.

Screening of small molecules enhancing endogenous miR-384-5p expression

Through a screening using an in-house small-molecule library that mainly comprised commercially available inhibitors of six kinase subfamilies [28], a small molecule that upregulated endogenous miR-384-5p was identified. Among the small molecules tested, small molecule number 145 (Drug 145; D145) most significantly increased miR-384-5p in CFs (Fig. 5a), and the identity of D145 was azathioprine, a well-known immunosuppressive agent [29]. To visualize D145-induced expression of miR-384-5p, Cy3-modified molecular beacons specific to miR-384-5p were used (Fig. 5b). When molecular beacon loaded CFs were treated with 10 μM D145 for 48 h, Cy3 signal in CFs prominently increased (Fig. 5c), indicating that D145 increased miR-384-5p in CFs. When the cells were treated with increasing concentrations of D145 (1, 2.5, 5, and 10 μM), the expression of miR-384-5p was significantly increased at concentrations of 2.5 μM or higher (Fig. 5d).

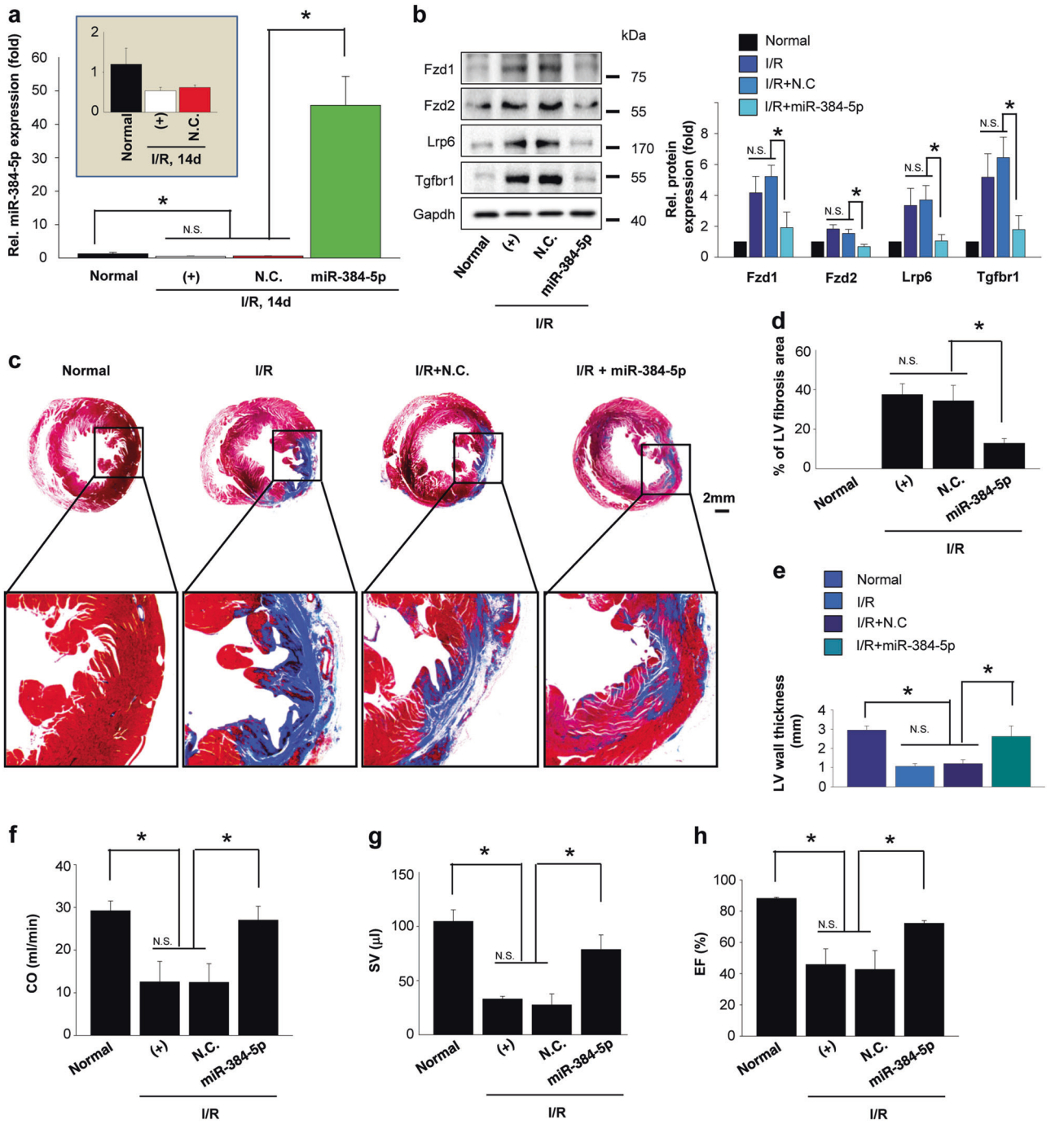

Fig. 4 MiR-384-5p attenuates cardiac fibrosis following I/R-injury. **a** The change in miR-384-5p expression following I/R-injury (14 days after the injury) was detected by real-time PCR. Inset figure: miR-384-5p expressions among the normal, I/R, and I/R + N.C. groups were compared, $*p < 0.05$. **b** The effect of exogenous miR-384-5p on the expression of the key receptors (Fzd-1, Fzd-2, Lrp6, and Tgfbr1) following I/R-injury (7 days after the injury) was detected by western blotting. $*p < 0.05$ compared to the I/R-injured group. **c** Representative images of Masson's trichrome-stained sections demonstrating fibrosis. **d** The area of fibrosis and **e** left ventricular (LV) wall thickness were measured. $*p < 0.05$. **f** Two weeks after the injury, cardiac output (CO) was measured to assess the effect of miR-384-5p administration on cardiac function, along with (**g**) systemic volume (SV) and **h** ejection fraction (EF). $*p < 0.05$. Quantitative data were expressed as the mean ± S.E.M. of the data collected from 5 animals. N.S not significant

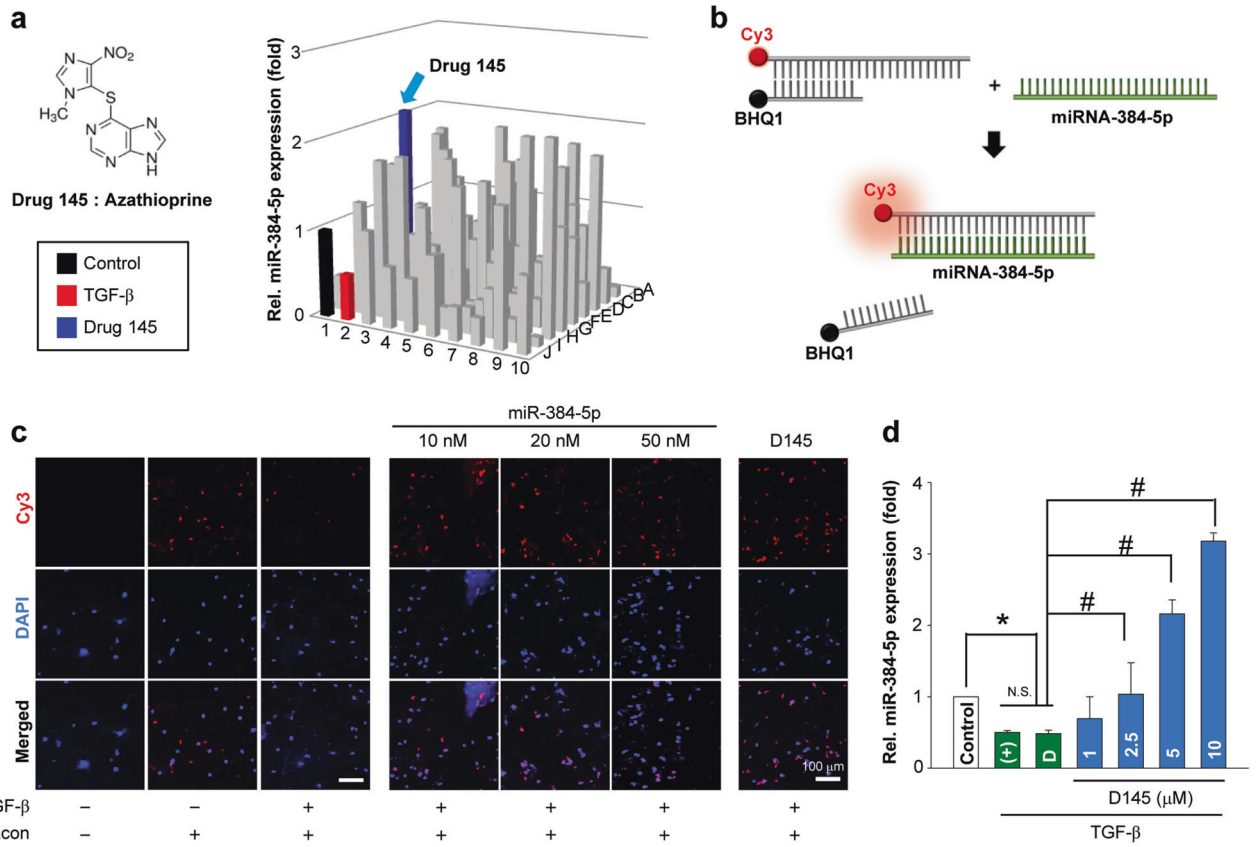

Fig. 5 Screening of a small molecule that increases endogenous miR-384-5p expression. **a** Primary CFs were treated with an in-house small-molecule library that mainly consisted of commercially available inhibitors of six kinase subfamilies (10 μM each) for 48 h. The expression level of miR-384-5p was determined by real-time PCR. **b** The schematics shows the working mechanism of the molecular beacon for detecting miRNA expression. **c** Left panel: to visualize the effect of TGF-β on the expression level of endogenous miR-384-5p, the cells were treated with or without TGF-β for 48 h. The Cy3-fluorescence, which indicates the presence of endogenous miR-384-5p, was detected. Right panel: the cells were treated with either increasing concentrations of miR-384-5p or 10 μM D145 as indicated for 48 h, and the Cy3-fluorescence from miR-384-5p bound molecular beacon was detected by using a confocal microscope . **d** The cells were treated with increasing concentrations of D145 in the presence of TGF-β (5 ng/ml) as indicated for 48 h. The expression level of miR-384-5p was determined by real-time PCR $^{*}p < 0.05$ compared to the untreated control, $\#p < 0.05$ compared to the TGF-β-treated group. Quantitative data were expressed as the mean ± S.E. M. of at least 3 independent experiments. N.S not significant,

D145 suppresses the expression of Fzd1, Fzd2, Tgfbr1, and Lrp5 and activation of TGF-β and Wnt/β-catenin signaling

Whether the D145-induced increase of miR-384-5p could be translated into actual downregulation of the receptors of interest was examined. D145 significantly decreased the expressions of Fzd1, Fzd2, Tgfbr1, and Lrp6 (Fig. 6a). Importantly, the effect of D145 was abrogated by anti-miR-384-5p treatment, demonstrating that the effect of D145 was due to enhanced expression of endogenous miR-384-5p. Next, the effect of D145 on TGF-β and Wnt signaling pathways was examined. D145 inhibited nuclear translocation of pNF-kB (Fig. 6b) and Smad pathway (Fig. 6c). Also, D145 decreased phosphorylation of GSK3β^{ser9} (Fig. 6d) and attenuated TGF-β-induced nuclear translocation of β-catenin (Fig. 6e). These results indicated that the effect of D145 was similar to that of exogenous miR-384-5p.

D145 attenuates TGF-β-induced CF activation

D145 significantly decreased the expression of collagen type I (Fig. 7a) and α-SMA (Fig. 7b), indicating that TGF-β-induced CF activation was significantly attenuated by D145. Furthermore, D145 significantly suppressed migration (Fig. 7c) and collagen contractility (Fig. 7d) of TGF-β-treated CFs. D145 also significantly attenuated the increase of CF proliferation following TGF-β treatment. However, such anti-proliferative effect of D145 was abrogated by anti-384-5p (Supplementary Fig. 9), indicating that even the anti-proliferative effect of D145 was miR-384-dependent.

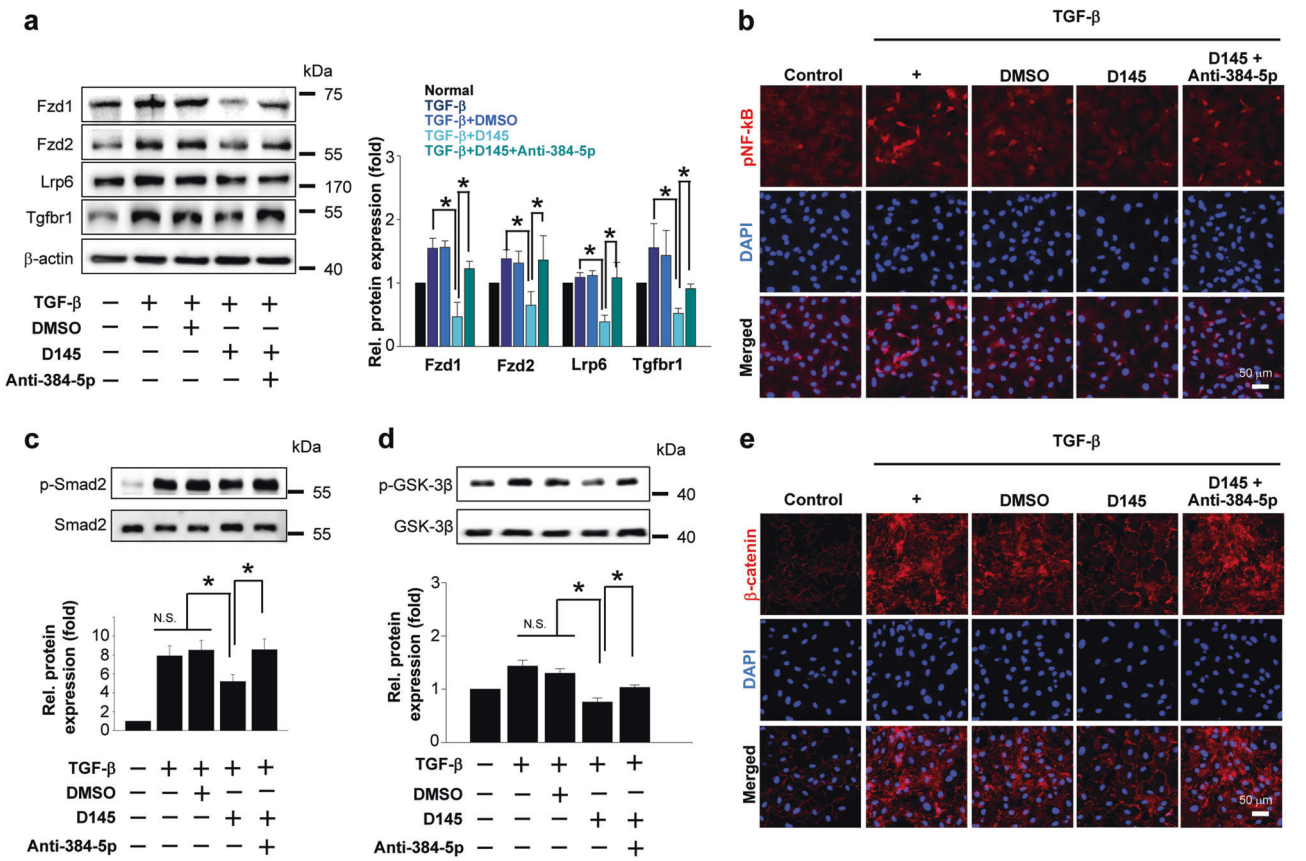

Fig. 6 D145 suppresses the expression of Fzd1, Fzd2, Tgfbr1, and Lrp5 and activation of TGF-β and Wnt/β-catenin signaling. **a** The cells were treated with 10 μM D145 for 24 h with or without the anti-miR-384-5p pretreatment. The expression of key receptors (Fzd1, Fzd2, Tgfbr1, and Lrp6) was examined by western blotting. $*p < 0.05$. **b** Nuclear translocation of pNF-kB was detected by using immunocytochemistry. Nuclei were stained with DAPI. **c** The expression levels of p-Smad was examined, $*p < 0.05$. **d** The expression levels of p-GSK3β was examined. $*p < 0.05$. Quantitative data were expressed as the mean ± S.E.M. of at least 3 independent experiments. **e** The cells were treated with 10 μM D145 for 24 h with or without the anti-miR-384-5p pretreatment. The expression level of β-catenin was visualized by immunocytochemistry. Nuclei were stained with DAPI. N.S not significant

D145 attenuates cardiac fibrosis following I/R-injury

D145 was intravenously (i.v.) injected via tail vein immediately after I/R-injury at a concentration of 10 μM (The whole blood volume of an individual rat was approximated as 7% of the body weight) [30]. The expression of miR-384-5p in the D145-treated group was well maintained for 2 weeks after the injury (Fig. 8a). To evaluate any organ-specific and/or general toxicity, multiple organs were weighed [31], and the weights were not significantly affected by D145, suggesting no serious in vivo adverse effects or toxicity of D145 (Fig. 8b). Next, the expressions of Fzd1, Fzd2, Tgrbr1, and Lrp6 were significantly suppressed by D145 (Fig. 8c). Most importantly, D145 significantly attenuated cardiac fibrosis (Fig. 8d), significantly decreasing the size of the fibrotic area (Fig. 8e) and preserving the LV wall thickness (Fig. 8f). D145 also significantly improved cardiac output, systemic volume, and ejection fraction (Fig. 8g). Taken altogether, D145 significantly suppressed cardiac fibrosis by preventing the decrease of miR-384-5p in the heart following I/R-injury.

Discussion

Previous studies have provided circumstantial evidence of a fibrogenic cross-talk between TGF-β and Wnt pathways by demonstrating that they can mutually activate each other in diseases involving myoFB formation [8–10]. Nevertheless, existence of such a transactivation circuit has not been examined nor experimentally confirmed in CF activation. In this study, we verified that those two pathways were indeed linked by demonstrating that exogenous TGF-β increased the production of Wnt3a in an NF-kB-dependent manner (Fig. 1c) and that both neutralization of Wnt3a (Fig. 1d) and suppression of Wnt/β-catenin signaling (Fig. 1e) disrupted the TGF-β auto-positive feedback loop. Thus, the present

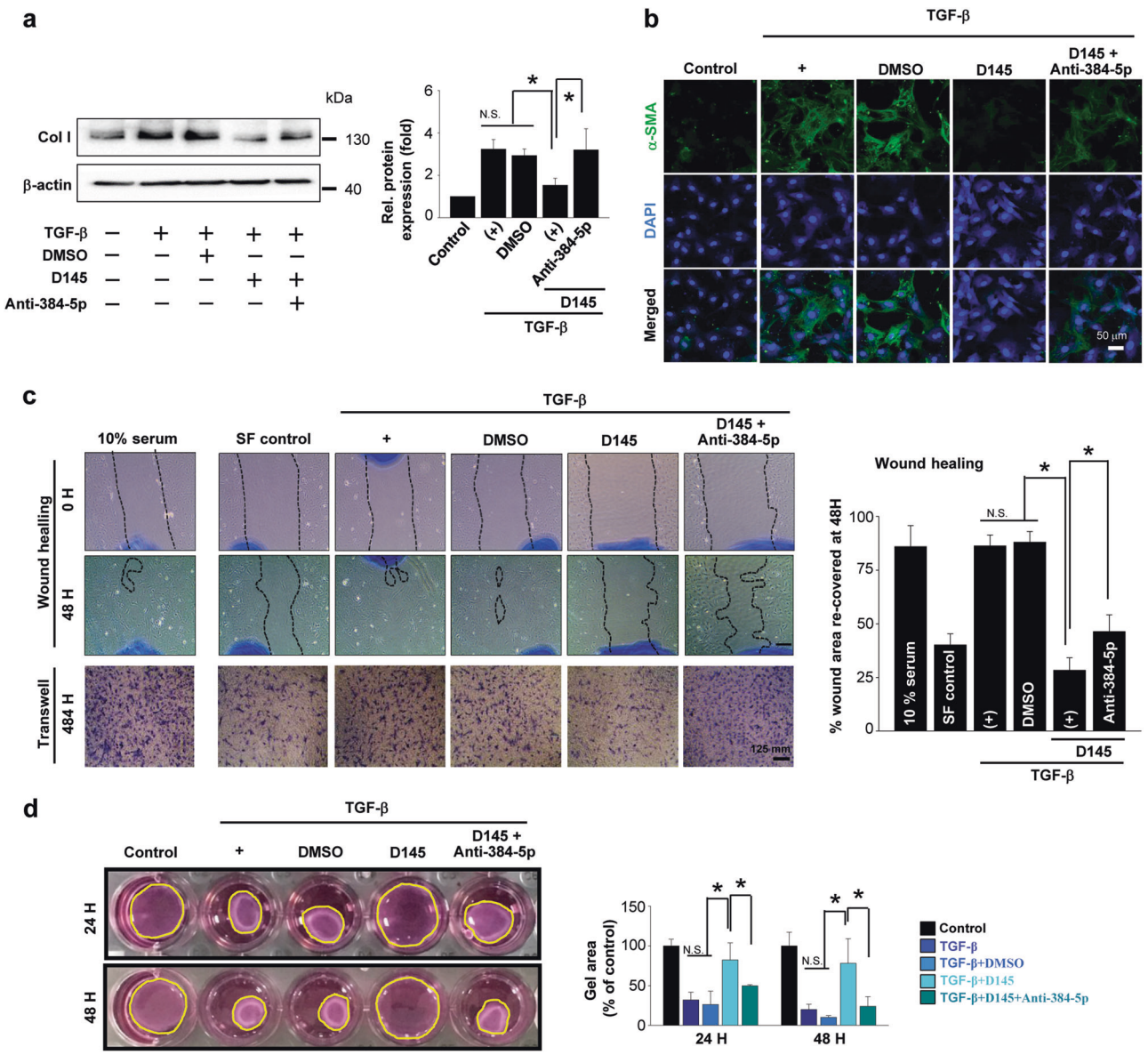

Fig. 7 Drug 145 attenuates TGF-β-induced CF activation. **a** The cells were treated with 10 μM D145 for 24 h with or without the anti-miR-384-5p pretreatment. The expression of collagen type I (Col I) was examined by western blotting, $*p < 0.05$. **b** The cells were treated with 10 μM D145 for 24 h with or without the anti-miR-384-5p pretreatment. The expression of α-SMA was visualized by immunocytochemistry. Nuclei were stained with DAPI. **c** For the wound-healing analysis, the cells were treated with 10 μM D145 for 48 h with or without the anti-miR-384-5p pretreatment. The images of the wound were obtained at 0 and 48 h. The area between the wound edges was measured and compared among the groups (right panel). $*p < 0.05$. For the migration analysis, the cells were seeded in the upper chambers of Transwells and treated with 10 μM D145 for 24 h with or without the anti-miR-384-5p pretreatment. The cells were further treated with TGF-β for an additional 24 h. The migrated cells were stained with crystal violet. **d** CF-containing collagen gels were serum-starved for 12 h. After 12 h, gels were stimulated with TGF-β (5 ng/ml) with or without D145 for 48 h and photographed at 24 h and 48 h. The sizes of the gels were measured and analyzed. $*p < 0.05$. Quantitative data were expressed as the mean ± S.E.M. of at least 3 independent experiments

study is the first to report the existence of a TGF-β/Wnt transactivation circuit (hereafter referred to as the circuit) in TGF-β-induced activation of CF. However, a thorough verification of the circuit, especially in vivo, would be extremely challenging because of other growth factors and cytokines [32, 33], which may affect the circuit. Therefore, providing direct in vivo evidence for a functioning circuit remains an issue that should be fully addressed in further studies.

Another significant finding of this study is the identification of miR-384-5p as an important regulator of the circuit. Our data suggested that miR-384-5p enhanced the expressions of key receptors (i.e., Fzd1, Fzd2, Tgfbr1, and Lrp6 in the present study) by being decreased in response to

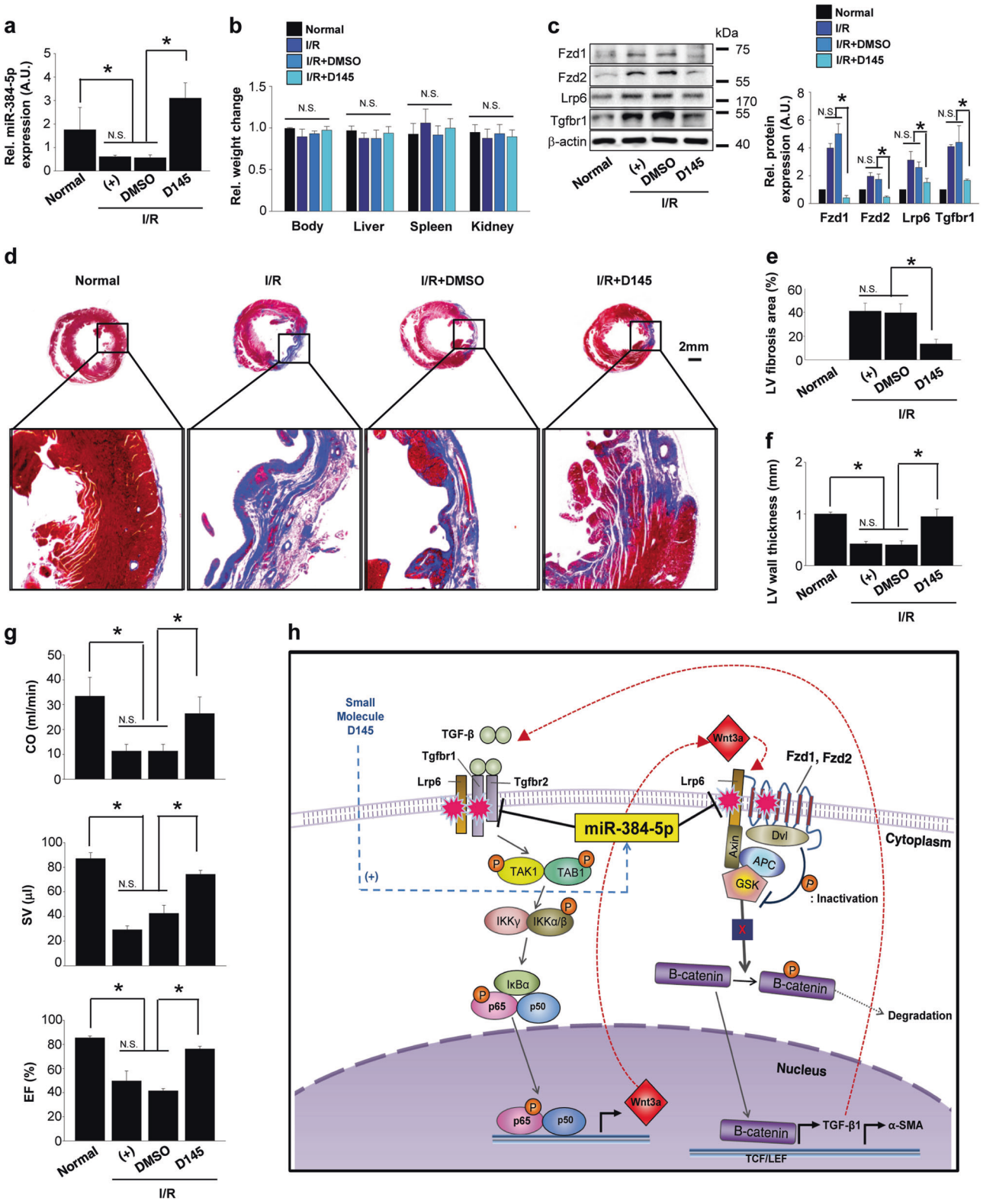

fibrogenic stimuli (Fig. 2e). The increased key receptors initiate and maintain the circuit, contributing to the progression of cardiac fibrosis. This speculation was indirectly verified by the observations of miR-384-5p-mediated suppression of CF activation in vitro (Fig. 3) and of improved cardiac function with attenuated cardiac fibrosis in vivo (Fig. 4). However, the present study did not cover the underlying mechanism of how fibrogenic stimuli

◀ **Fig. 8** D145 attenuates cardiac fibrosis following I/R-injury. **a** The change in miR-384-5p expression following I/R-injury (14 days after the injury) with i.v. injection of D145 was detected by real-time PCR, $*p < 0.05$. **b** The body and organ (liver, spleen, and kidney) weight were measured to evaluate the general and organ-specific toxicity of D145. The organs were collected and weighed upon sacrifice of the animals at the end of the study. **c** The expression levels of key receptors in the I/R-injured heart with i.v. injection of D145 were detected by western blotting. $*p < 0.05$. **d** Representative images of Masson's trichrome-stained sections demonstrating fibrosis. **e** The area of fibrosis and **f** left ventricular (LV) wall thickness were measured. **g** Two weeks after the injury, cardiac output (CO), systemic volume (SV), and ejection fraction (EF) were measured to assess the effect of D145 administration on cardiac function. $*p < 0.05$. Quantitative data were expressed as the mean ± S.D. of the data collected from 5 animals. **h** Model depicting miR-384-5p-mediated regulation of the TGF-β/Wnt transactivation circuit in CFs. The expression level of endogenous miR-384-5p is reduced by fibrogenic stimuli, increasing the expression of the key receptors (Fzd1, Fzd2, Lrp6, and Tgfrb1). This increase augments TGF-β-induced expression of the Wnt ligand Wnt3a, and consequently, Wnt3a further increases TGF-β production, establishing a TGF-β/Wnt transactivation circuit during CF activation. Small-molecule D145 augments the expression of endogenous miR-384-5p under fibrogenic stimuli, disrupting the transactivation circuit. N.S not significant

downregulate miR-384-5p expression, and it remains to be one of the limitations of the present study.

Regarding the two miRNAs predicted to target the key receptors of the circuit (Fig. 2a), miR-384-5p is reportedly downregulated in ischemic diseases and in failing heart [34–36], whereas increased expression of miR-141-3p following ischemic preconditioning has been reported [37], supporting the legitimacy of choosing miR-384-5p over miR-141-3p as a key miRNA that regulates the circuit. Regarding the role of miR-384-5p in cardiovascular disease, one study reported that miR-384-5p exerted a pro-apoptotic effect in cardiomyoblasts in vitro [38]. This particular study claimed that miR-384-5p increased the expression of caspase 3 and decreased the viability of cardiomyoblasts. However, it did not clearly indicate the concentration of miRNA mimics used, making it difficult to evaluate and generalize their findings. We can only speculate that the observed effect of miR-384-5p was cell-type specific or that the effect was an artifact caused by an improper concentration of miRNA mimics. Interestingly, even the aforementioned study demonstrated that the expression of miR-384-5p decreased by 60% in the ischemic myocardium. To better comprehend the role of miR-384-5p in the cardiovascular system, investigating the effects of miR-384-5p on different types of cardiac cells other than fibroblasts will be a good subject for further studies.

The most clinically relevant finding of this study is the prevention of cardiac fibrosis mediated by D145. To bypass current limitations of direct in vivo delivery of miRNAs, such as low cellular uptake, off-target effects, and instability in serum [39], small-molecule-mediated regulation of endogenous miR-384-5p was utilized as an alternative strategy to modulate the expressions of key receptors involved in the circuit in vivo. The selected small molecule D145 significantly attenuated TGF-β-induced downregulation of miR-384-5p (Fig. 5d) and suppressed TGF-β-induced activation of CFs in vitro (Fig. 7). However, our unpublished data showedd that D145 at a higher concentration (> 10 μM) failed to further enhance the expression of miR-384-5p, suggesting that D145 may act on saturable target(s) such as enzymes involved in miR-384-5p biosynthesis. Unfortunately, the exact mechanism still remains elusive and we are currently conducting a further study specifically aimed to identify the underlying mechanisms of miR-384-5p regulation by D145 and fibrogenic stimuli such as TGF-β.

In addition to suppressing TGF-β-induced activation of CFs in vitro, D145 significantly attenuated cardiac fibrosis and improved cardiac function following I/R-injury in vivo (Fig. 8). Although the D145-mediated recovery of endogenous miR-384-5p in the presence of fibrogenic stimuli (Fig. 8a) and downregulation of the key receptors (Fig. 8c) following I/R-injury indicated that the anti-fibrotic effect of D145 was mediated by the disruption of the circuit as proposed, additional unforeseen mechanisms may function in vivo. Unlike in vitro conditions where biological variables are relatively well-controlled and minimized (e.g., single cell type and single treatment) in vivo condition includes a wide variety of cells and a number of soluble factors. Therefore, unexpected mechanism(s) of action may also contribute to the outcomes of an in vivo experiment. Therefore, an overview of other plausible mechanisms that might have contributed to the observed anti-fibrotic effect of D145 is required to interpret the outcomes correctly and to design further in vivo studies adequately.

The very first possibility is that the downregulation of Wnt signaling has anti-fibrogenic effects on cardiac cells other than CFs [40]. Downregulation of β-catenin enhances resident precursor cell differentiation and attenuates ischemic cardiac remodeling [41], and a small-molecule inhibitor of Wnt signaling improves the contractile function in the infarcted heart [42]. Furthermore, blocking Fzd-mediated Wnt signaling by using either a soluble decoy for the Wnt protein [43] or siRNA-that is specific to Fzd [44] prevented apoptosis of cardiomyocytes, supporting the possibility that D145 acts as a regulator of a Wnt-based niche in the I/R-injured heart.

Another possibility is based on the pharmaceutical nature of D145. The identity of D145 is azathioprine, a well-known immunosuppressive agent [29]. The immunosuppressive effect of azathioprine is achieved via inhibition of CD28-mediated signaling [45]. CD28 is a homodimeric stimulatory receptor that is expressed on T cells and mediates co-stimulation of T cells [46]. Recently, studies have

reported that inhibition of T-cell co-stimulation [47] or CD28 deficiency [48] has a protective effect on pressure overload-induced congestive heart failure. Therefore, D145 may have protected the I/R-injured heart by not only disrupting the circuit but by also suppressing the immune response following I/R-injury. Additionally, as a purine analogue, D145 inhibits the DNA replication in rapidly dividing cells, such as lymphocytes, and TGF-β is also released by infiltrating lymphocytes [49]. Therefore, it is also possible that D145 decreased the overall production of TGF-β following I/R injury by inhibiting the proliferation of infiltrated lymphocytes. However, these possibilities will remain speculative until they are experimentally confirmed.

The present study has provided strong evidence of a TGF-β/Wnt transactivation circuit in CFs and identified miR-384-5p as a key regulator of the circuit (Fig. 8h). In the clinical context, it was demonstrated that modulating a key miRNA targeting multiple fibrogenic mediators can be an effective means to control cardiac fibrosis and that small-molecule-mediated regulation of endogenous miRNA has significant therapeutic potential as a clinically viable alternative to direct application of exogenous miRNAs. To fully address the unanswered issues, further studies are warranted.

Methods

Isolation of neonatal rat CFs

The hearts of 8-week-old Sprague–Dawley rat pups were used for the study. The extracted ventricle was washed with Dulbecco's phosphate-buffered saline (DPBS) solution (pH 7.4, Gibco BRL, Grand Island, NY, USA) without Ca^{2+} and Mg^{2+}. Using micro-dissecting scissors, hearts were minced to pieces of approximately 1 mm^3 and treated with 10 ml of collagenase II (0.8 mg/ml, 262 units/mg, Gibco BRL, Grand Island, NY, USA) for 5 min at room temperature. The initial supernatant was discarded by decantation and the remained tissues were treated with fresh collagenase II solution for an additional 5 min at 37 °C. The supernatant containing cells was transferred to a tube containing cell culture medium (DMEM/F-12 containing 10% fetal bovine serum, Gibco BRL, Grand Island, NY, USA), and centrifuged at 1200 r.p.m. for 4 min at room temperature. The cell pellets were re-suspended in 5 ml of cell culture medium. The above procedures were repeated 7–9 times until little tissues were left. The cell suspensions were collected and incubated in 100 mm tissue culture dishes for 30 min for attachment. Unattached cells were discarded by changing culture medium. Attached fibroblasts were then cultured with DMEM/F-12 containing 10% (v/v) FBS in a CO2 incubator at 37 °C. CFs with passages between 1 and 3 were used for all studies.

Cell proliferation assay

CFs were treated with 10 μM of D145 for 48 h with or without the anti-miR-384-5p pretreatment in a 96 well plate. Relative cell proliferation was determined by using cell counting kit (CCK, Dojindo, Japan). Briefly, WST-8 [2-(2-methoxy-4-nitrophenyl)-3-(4-nitrophenyl)-5-(2,4-disulfophenyl)-2H-tetrazolium, monosodium salt] solution (1:10, v/v) was added to each well and incubated at 37 °C for 2 h to allow formation of WST-8 formazan. The Absorbance of a water soluble formazan dye was measured at 450 nm.

MicroRNA transfection

MicroRNAs and scrambled RNA oligomer (negative control scrambled miRNA, N.C.) were purchased from Genolution Inc. (Seoul, Korea). Transfection of microRNAs was performed using a TransIT-X2 system (Mirus Bio LLC, Madison, WI, USA). Briefly, cells were seeded at a density of 7×10^5 cells per 60 mm culture plates. The TransIT-X2 reagent was diluted with Opti-MEM and combined with microRNA mimics. The mixture was added to each well. After 24 h of incubation in a CO2 incubator at 37 °C, the medium was changed to fresh 10% FBS DMEM.

Reverse transcription polymerase chain reaction (RT-PCR)

Total RNA was extracted using TRIzol (Sigma-Aldrich, St Louis, MO, USA, 500 μL per 60 mm culture dish). Chloroform (100 μL) was added to the extract and each sample was vortexed for 15 s. The mixtures were centrifuged at 12,000 r.p.m. for 15 min at 4 °C, and the transparent upper layer was collected in a new tube. Each sample was mixed with 300 μL of isopropanol. The samples were centrifuged at 12,000 r.p.m. for 10 min at 4 °C. The supernatant was discarded and the pellet was washed using 75% (v/v) ethanol. The samples were centrifuged at 12,000 r.p.m. for 5 min at 4 °C, and the supernatant was discarded. The pellet was air-dried at room temperature, and dissolved in 20 μL of nuclease-free water. Complementary DNA (cDNA) was generated using 500 ng of total RNA with AccuPower PT PreMix (Bioneer, Seoul, Korea) according to the manufacturer's instructions. The PCR conditions consisted of denaturing at 94 °C for 3 min, followed by 25 cycles of denaturation at 94 °C for 30 s, annealing at 55 °C for 30 s, and extension at 72 °C for 30 s, before a final extension at 72 °C for 10 min. PCR products were separated by electrophoresis in 1.2% (w/v) agarose gels (Bio-Rad, Hercules, CA, USA). Glyceraldehyde-3-phosphate dehydrogenase (Gapdh) was used as an internal standard.

Real-time polymerase chain reaction (Real-time PCR)

Total RNA extraction procedure was identical to that of RT-PCR. cDNA was generated using 10 ng of purified total RNA with Taqman® MicroRNA Reverse Transcriptase Kit (Applied Biosystems, Foster City, CA, USA) in combination with Taqman® MicroRNA Assays. For normalization, U6 control transcripts were used. Amplification and detection of specific products were performed in a Step One plus Real-Time PCR system (Applied Biosystems, Foster City, CA, USA) at 95 °C for 10 min, followed by 40 cycles of 95 °C for 15 s and 60 °C for 60 s.

Luciferase reporter assay

The 3'UTR fragment of each targeted gene (covering 50 bp upstream and 50 bp downstream of the miR-384-5p-binding sequence) was used for luciferase assay. Approximately 120 bp-long 3′-UTR fragment of each target was PCR amplified by using primers containing XhoI (forward) and SalI (Reverse) enzyme site. The PCR product was then cloned into pmirGLO Dual Luciferase vector (Promega, Madison, WI, USA) using the XhoI and SalI enzyme site. For transfection, Hela cells were seeded in 24-well plate at a density of 5×10^4 cells/well. When the cells reached confluency of near 80%, 500 ng of pmirGLO vectors containing the 3'UTR fragment was transfected by using lipofectamin LTX system (Invitrogen, Carlsbad, CA, USA) according to the manufacturer's recommendation. 24 h after the transfection, luciferase activity was measured using Dual-luciferase reporter assay system (Promega, Madison, WI, USA). The Renilla luciferase was used to normalize the cell number and the transfection efficiency.

Promoter assay

The promoter region of rno-miR-384-5p from -1 up to -3000 was amplified using KpnI site containing forward primers containing set of 5′-AAGGTACCATAGATC TGTAATAACTC-3′ (1000 bp fragment, F1), 5′-AAGGTA CCTTCTCAGCTAACCAGCTC-3′ (1,250 bp fragment, F2), 5′-AAGGTACCGAGAGCAGTGTAGAGCTC-3′ (1,500 bp fragment, F3), 5′-AAGGTACCAAGAG AGTGTATACCAT-3′ (1,750 bp fragment, F4), 5′-AAGG TACCGTATGTTTAGCTTTCT TT-3′ (2000 bp fragment, F5), and 5′-AAGGTACCGGTACTCTTCATTTCTTT-3′ (3000 bp fragment, F6). For XhoI site containing reverse primer, 5′-AACTCGAGTAACATTTCGCTGCAACA-3′ was used. PCR amplicons were digested with KpnI and XhoI, and inserted into the pGL3-basic vector (Promega, Madison, WI, USA). For transfection, HeLa cells were seeded in 24-well plate at a density of 5×10^4 cells/well. When the cells reached confluency of near 80%, 500 ng of pGL3 vectors containing the promoter fragment was transfected by using lipofectamin LTX system (Invitrogen, Carlsbad, CA, USA) according to the manufacturer's recommendation. 24 after the transfection, luciferase activity was measured.

Western blot

The cells were washed in PBS and lysed in lysis buffer (Cell Signal Technology, Danvers, MA, USA). Protein concentrations were determined using the BCA Protein Assay Kit (Thermo Fisher Scientific, Waltham, MA, USA). Equal amount of proteins were separated in a sodium dodecyl sulfate-polyacrylamide gel (SDS-PAGE) and transferred to a polyvinylidene difluoride membrane (Millipore, Billerica, MA, USA). After blocking the membrane by using Tris-buffered saline-Tween 20 (TBS-T, 0.05% Tween 20) and 10% skim milk for 1 h at room temperature, the membranes were incubated with appropriate primary antibodies. Antibodies specific to α-SMA and β-actin were purchased from Abcam (Cambridge, UK), and the following antibodies were purchased from Cell Signaling Technology (Danvers, MA, USA): Collagen type I, p-JNK, JNK, p-GSK-3β, GSK-3β, p-P65, P65, p-P38, p38, p-IKKα, Fzd1, Lrp6, p-Smad and Smad. Antibodies specific to Collagen type III, p-CamK II, CamK II, β-catenin, p-TAK1, Wnt3a, TGF-β, and Tgfbr1 were from Santa Cruz Biotechnology (Dallas, TX, USA). Additionally, antibodies specific to Lamin B2 (Invitrogen, Carlsbad, CA, USA) and Fzd-2 (OriGene, Rockville, MD, USA) were also used. After incubation with appropriate antibodies overnight at 4 °C, the membrane was washed three times with 0.05% TBS-T for 10 min each and then incubated for 1 h at room temperature with horseradish peroxidase-conjugated secondary antibodies. The immune-positive bands were detected by an enhanced chemiluminescence (ECL) reagent (Santa Cruz Biotechnology, Dallas, TX, USA). The band intensities were quantified using NIH Image J version 1.34e software.

Nuclear and cytoplasmic extraction

For nuclear and cytoplasmic extraction, NE-PER Nuclear and Cytoplasmic Extraction Reagents (Thermo Fisher Scientific, Waltham, MA, USA) were used according to the user manual provided by the manufacturer.

NFkB p65 transcription factor assay

To assess the transcription factor p65 binding, a NFkB p65 transcription factor assay kit (Abcam, Cambridge, UK) was used according to the user manual provided by the manufacturer. Briefly, the cells were transfected with 100 nM of either miR-384-5p or anti-miR-384-5p for 24 h, and then

exposed to 5 ng/ml TGF-β for 1 h. Nuclear extracts (5 µg) were used to determine the binding of NF-κB p65 in each group.

Immunocytochemistry

CFs were cultured in four-well slide chambers at a density of 2.2×10^4. The cells were permeabilized using 0.1% Triton X-100 for 10 min. Next, the cells were blocked for 1 h in a blocking solution (2% bovine serum albumin and 10% horse serum in PBS) and incubated with α-SMA (Abcam, Cambridge, UK), Vimentin (Abcam, Cambridge, UK), vWf (Santa Cruz Biotechnology, Dallas, TX, USA), p65 (Cell Signaling Technology, Danvers, MA, USA) and β-catenin antibodies (Santa Cruz Biotechnology, Dallas, TX, USA). FITC-conjugated mouse and rabbit secondary antibodies (Jackson ImmunoResearch Laboratories, West Grove, PA, USA) were used. Immunofluorescence was detected by a confocal microscope (LSM710; Carl Zeiss Microscopy GmbH, Jena, Germany).

Immunohistochemistry

To identify fibroblast, rat monoclonal ER-TR7 antibodies (Santa Cruz Biotechnology, Dallas, TX, USA) were used and rabbit polyclonal CD68 antibodies (Abcam, Cambridge, UK) were used as a macrophage marker. For detection of Wnt3a and Wnt5a, Alexa Fluor 488 conjugated mouse monoclonal Wnt3 antibodies (Santa Cruz Biotechnology, Dallas, TX, USA) and mouse monoclonal Wnt5a antibodies (Santa Cruz Biotechnology, Dallas, TX, USA) were used, respectively. In brief, I/R-injured heart sections (7d) were blocked in 2.5% normal horse serum and incubated overnight with respective antibodies at 4 °C. Texas red- conjugated anti-rat IgG (Jackson Immuno Research Laboratories, West Grove, PA, USA) or FITC-conjugated anti-rabbit IgG (Jackson Immuno Research Laboratories, West Grove, PA, USA) was used as secondary antibody.

Co-localization Image analysis

The degree of co-localization was measured by ZEN 2009 Light Edition software that calculated the percentage of co-localized pixels relative to all pixels obtained. Following Carl Zeiss Micro-imaging, the Pearson's correlation coefficient R (PCC) value was calculated. The value for PCC can range from -1 to 1, and a value of 1 indicates that the fluorescence patterns of the two molecules are perfectly matched [50].

Wound healing assay

CFs were plated at a density of 2.5×10^5 cells/well in six-well plates. When the cells reached 90% confluence, cells were starved for 12 h. After starvation, scratches were produced with 200 µl pipette tips and images were captured using an Axiovert 40 C inverted microscope (Carl Zeiss Microscopy GmbH, Jena, Germany) equipped with a Powershot A640 digital camera (Canon, Tokyo, Japan). The medium was replaced with or without small molecule and TGF-β. The migrated area was captured at 0, 24, or 48 h after the TGF-β-treatment and the percent of area re-covered by growth was calculated.

Transwell migration assay

CFs (0.6×10^4cells) were plated in the upper chamber of Transwell assay plates with 8 µm filter pore size (Costar Corning, Corning, NY, USA). The cells were incubated in serum deprivation media for 12 h, and small molecule was added to upper chamber. After 1 h, TGF-β was added to the bottom chamber, and incubated at 37 °C for 24 h. After incubation, the migrated cells were stained with 0.25% crystal violet. Non-migrated cell on the inside of the upper chamber were removed with cotton swabs.

Collagen gel contraction assay

CFs were transfected miR-384-5p or anti-miR-384-5p at concentration 100 nM and 50 nM, respectively, for 24 h. After additional 24 h of incubation in culture media containing 10% FBS, the cells were re-suspended in medium at a density of 3×10^6 cells/ml. Subsequently, 100 µl cell suspension was mixed with 400 µl collagen solution (Sigma-Aldrich, St Louis, MO, USA) and 1 M NaOH. Five hundred µl of the mixture was caste into 24-well cell culture plates and incubated at 37 °C for 1 h for polymerization. After 1 h, 600 µl of DMEM was added to each well, and gels were released from the surface of the plate by using a pipette tip. Drug 145 was pretreated for 1 h and TGF-β (5 ng/ml) was added.

Antibody neutralization assay

CFs (2.2×10^5 cells) were plated in 6-well culture plates. Wnt3a-neutralizing antibodies or IgG control antibodies (15 ug/ml, each). were added to appropriate wells 1 h prior to TGF-β treatment. After 24 h of TGF-β treatment, cells were lysed for western blot analysis.

Detection of miR-384-5p using molecular beacon

Molecular beacons for detecting miR-384-5p were prepared by annealing Cy3-modified long sequence (Cy3-ACATT TATTAAGGATCCGTTACA) and black hole quencher (BHQ1) modified short sequence (BHQ1-TGTAAA TAAT). After seeding CFs in 96 well culture plates, the

cells were treated with 10 μM of D145 or transfected with increasing concentrations of miR-394-5p (10, 20, and 50 nM) for 48 h. To detect miR-384-5p, molecular beacons were delivered to CFs at a concentration of 50 nM using a lipofectamin LTX system. After 24 h after the molecular beacon delivery, Cy3 fluorescence was detected by using a confocal microscope (LSM710; Carl Zeiss Microscopy GmbH, Jena, Germany).

Rat cardiac ischemia/reperfusion (I/R) injury model

All experimental procedures for animal studies were approved by the Committee for the Care and Use of Laboratory Animals, Yonsei University College of Medicine, and performed in accordance with the Committee's Guidelines and Regulations for Animal Care. I/R-injury was produced in male Sprague–Dawley rats (200 ± 50 g) by surgical occlusion of the left anterior descending coronary artery. Briefly, after induction of anesthesia with zoletil (0.8 ml/kg) and rompun (0.2 ml/kg), the rats were intubated, and ventilation (62 strokes/min, tidal volume 8–10 ml/kg) was maintained using a Harvard ventilator (Holliston, MA, USA). After intubation, the third and fourth ribs were cut to open the chest, and the heart was exteriorized through the intercostal space. The left coronary artery was then ligated 2–3 mm from its origin with a 6-0 prolene suture (Ethicon, Somerville, NJ, USA). Reperfusion was conducted after 1 h of ischemia. For transplantation, microRNA (10 μg/head) and reagent mixture were prepared in 60 μl and injected from the injured region to the border using a Hamilton syringe (Hamilton Co., Reno, NV, USA) with a 30 gauge needle. For drug injection, D145 was intravenously (i.v.) injected right after I/R-injury at concentration of 10 μM (whole blood volume of an individual rat was approximated as 7% of body weight). Throughout the operation, animals were ventilated with 95% O_2 and 5% CO_2 using a Harvard ventilator (Holliston, MA, USA). For each group, 5 animals (ligation, miR-384-5p injection, Drug 145 injection, DMSO injection and Reagent injection) were used. Animals were sacrificed 1 to 2 weeks after the surgery for analysis, depending on experiments conducted.

Functional analysis of heart

For invasive hemodynamics, left ventricular catheterization was performed at 2 weeks after I/R and treatment. A Millar Micro-tip 2 F pressure transducer (model SPR-838, Millar Instruments, USA) was introduced into the left ventricle via the right carotid artery under zoletil (20 mg/kg) and xylazine (5 mg/kg) anesthesia. Real-time pressure volume loops were recorded and data were analyzed with PVAN 3.5 software (Millar).

Statistical analysis

Quantitative data are presented as mean ± S.E.M. of at least 3 independent experiments. For statistical analysis, Student's t test was used to compare two experimental groups, or one-way ANOVA with Bonferroni correction was performed using OriginPro 8 SR4 software (ver. 8.0951, OriginLab Corporation, Northampton, MA, USA) if there were more than 3 groups. A p value of less than 0.05 was considered statistically significant.

Acknowledgements This study was supported by grants funded by the Korea Ministry of Science, ICT and Future Planning (NRF-2015M3A9E6029519 and NFR-2015M3A9E6029407).

Compliance with ethical standards

Conflict of interest The authors declare that they have no conflict of interest.

References

1. Baum J, Duffy HS. Fibroblasts and myofibroblasts: what are we talking about? J Cardiovasc Pharmacol. 2011;57:376–9.
2. Talman V, Ruskoaho H. Cardiac fibrosis in myocardial infarction-from repair and remodeling to regeneration. Cell Tissue Res. 2016;365:563–81.
3. Chablais F, Jazwinska A. The regenerative capacity of the zebrafish heart is dependent on TGFbeta signaling. Development . 2012;139:1921–30.
4. Dobaczewski M, Chen W, Frangogiannis NG. Transforming growth factor (TGF)-beta signaling in cardiac remodeling. J Mol Cell Cardiol. 2011;51:600–6.
5. Meng XM, Nikolic-Paterson DJ, Lan HY. TGF-beta: the master regulator of fibrosis. Nat Rev Nephrol. 2016;12:325–38.
6. Leask A. TGFbeta, cardiac fibroblasts, and the fibrotic response. Cardiovasc Res. 2007;74:207–12.
7. Tao H, Yang JJ, Shi KH, Li J. Wnt signaling pathway in cardiac fibrosis: New insights and directions. Metabolism. 2016;65: 30–40.
8. Akhmetshina A, Palumbo K, Dees C, Bergmann C, Venalis P, Zerr P, et al. Activation of canonical Wnt signalling is required for TGF-beta-mediated fibrosis. Nat Commun. 2012;3:735.
9. Carthy JM, Garmaroudi FS, Luo Z, McManus BM. Wnt3a induces myofibroblast differentiation by upregulating TGF-beta signaling through SMAD2 in a beta-catenin-dependent manner. PLoS ONE. 2011;6:e19809.
10. Blyszczuk P, Muller-Edenborn B, Valenta T, Osto E, Stellato M, Behnke S, et al. Transforming growth factor-beta-dependent Wnt secretion controls myofibroblast formation and myocardial fibrosis progression in experimental autoimmune myocarditis. Eur Heart J. 2017;38:1413–25.
11. Ha M, Kim VN. Regulation of microRNA biogenesis. Nat Rev Mol Cell Biol. 2014;15:509–24.
12. Xu P, Guo M, Hay BA. MicroRNAs and the regulation of cell death. Trends Genet. 2004;20:617–24.
13. Ivey KN, Srivastava D. MicroRNAs as regulators of differentiation and cell fate decisions. Cell Stem Cell. 2010;7:36–41.
14. Hwang HW, Mendell JT. MicroRNAs in cell proliferation, cell death, and tumorigenesis. Br J Cancer. 2007;96(Suppl):R40–44.

15. Hashimoto Y, Akiyama Y, Yuasa Y. Multiple-to-multiple relationships between microRNAs and target genes in gastric cancer. PLoS ONE. 2013;8:e62589.
16. MacDonald BT, Tamai K, He X. Wnt/beta-catenin signaling: components, mechanisms, and diseases. Dev Cell. 2009;17:9–26.
17. Kikuchi A, Yamamoto H, Sato A, Matsumoto S. New insights into the mechanism of Wnt signaling pathway activation. Int Rev Cell Mol Biol. 2011;291:21–71.
18. Fredriksson R, Lagerstrom MC, Lundin LG, Schioth HB. The G-protein-coupled receptors in the human genome form five main families. Phylogenetic analysis, paralogon groups, fingerprints. Mol Pharmacol. 2003;63:1256–72.
19. Blankesteijn WM, Essers-Janssen YP, Verluyten MJ, Daemen MJ, Smits JF. A homologue of Drosophila tissue polarity gene frizzled is expressed in migrating myofibroblasts in the infarcted rat heart. Nat Med. 1997;3:541–4.
20. Laeremans H, Hackeng TM, van Zandvoort MA, Thijssen VL, Janssen BJ, Ottenheijm HC, et al. Blocking of frizzled signaling with a homologous peptide fragment of wnt3a/wnt5a reduces infarct expansion and prevents the development of heart failure after myocardial infarction. Circulation . 2011;124:1626–35.
21. Lin H, Angeli M, Chung KJ, Ejimadu C, Rosa AR, Lee T. sFRP2 activates Wnt/β-catenin signaling in cardiac fibroblasts: differential roles in cell growth, energy metabolism, and extracellular matrix remodeling. Am J Physiol Cell Physiol. 2016;311:C710–9.
22. Choi ME, Ding Y, Kim SI. TGF-beta signaling via TAK1 pathway: role in kidney fibrosis. Semin Nephrol. 2012;32:244–52.
23. Karin M. How NF-kappaB is activated: the role of the IkappaB kinase (IKK) complex. Oncogene . 1999;18:6867–74.
24. Natarajan K, Singh S, Burke TR Jr, Grunberger D, Aggarwal BB. Caffeic acid phenethyl ester is a potent and specific inhibitor of activation of nuclear transcription factor NF-kappa B. Proc Natl Acad Sci USA. 1996;93:9090–5.
25. Handeli S, Simon JA. A small-molecule inhibitor of Tcf/beta-catenin signaling down-regulates PPARgamma and PPARdelta activities. Mol Cancer Ther. 2008;7:521–9.
26. Shi Y, Massague J. Mechanisms of TGF-beta signaling from cell membrane to the nucleus. Cell . 2003;113:685–700.
27. MacDonald BT, He X. Frizzled and LRP5/6 receptors for Wnt/beta-catenin signaling. Cold Spring Harb Perspect Biol. 2012;4. https://doi.org/10.1101/cshperspect.a007880
28. Hwang KC, Kim JY, Chang W, Kim DS, Lim S, Kang SM, et al. Chemicals that modulate stem cell differentiation. Proc Natl Acad Sci USA. 2008;105:7467–71.
29. Maltzman JS, Koretzky GA. Azathioprine: old drug, new actions. J Clin Invest. 2003;111:1122–4.
30. Lee HB, Blaufox MD. Blood volume in the rat. J Nucl Med. 1985;26:72–6.
31. Michael B, Yano B, Sellers RS, Perry R, Morton D, Roome N, et al. Evaluation of organ weights for rodent and non-rodent toxicity studies: a review of regulatory guidelines and a survey of current practices. Toxicol Pathol. 2007;35:742–50.
32. Kendall RT, Feghali-Bostwick CA. Fibroblasts in fibrosis: novel roles and mediators. Front Pharmacol. 2014;5:123.
33. Borthwick LA, Wynn TA, Fisher AJ. Cytokine mediated tissue fibrosis. Biochim Biophys Acta. 2013;1832:1049–60.
34. Muthusamy S, DeMartino AM, Watson LJ, Brittian KR, Zafir A, Dassanayaka S, et al. MicroRNA-539 is up-regulated in failing heart, and suppresses O-GlcNAcase expression. J Biol Chem. 2014;289:29665–76.
35. Zhai F, Zhang X, Guan Y, Yang X, Li Y, Song G, et al. Expression profiles of microRNAs after focal cerebral ischemia/reperfusion injury in rats. Neural Regen Res. 2012;7:917–23.
36. Sun G, Hu H, Tian X, Yue J, Yu H, Yang X, et al. Identification and analysis of microRNAs in the left ventricular myocardium of two-kidney one-clip hypertensive rats. Mol Med Rep. 2013;8:339–44.
37. Lee ST, Chu K, Jung KH, Yoon HJ, Jeon D, Kang KM, et al. MicroRNAs induced during ischemic preconditioning. Stroke . 2010;41:1646–51.
38. Bao Y, Lin C, Ren J, Liu J. MicroRNA-384-5p regulates ischemia-induced cardioprotection by targeting phosphatidylinositol-4,5-bisphosphate 3-kinase, catalytic subunit delta (PI3K p110delta). Apoptosis . 2013;18:260–70.
39. Pecot CV, Calin GA, Coleman RL, Lopez-Berestein G, Sood AK. RNA interference in the clinic: challenges and future directions. Nat Rev Cancer. 2011;11:59–67.
40. Hermans KC, Daskalopoulos EP, Blankesteijn WM. Interventions in Wnt signaling as a novel therapeutic approach to improve myocardial infarct healing. Fibrogenes Tissue Repair. 2012;5:16.
41. Zelarayan LC, Noack C, Sekkali B, Kmecova J, Gehrke C, Renger A, et al. Beta-Catenin downregulation attenuates ischemic cardiac remodeling through enhanced resident precursor cell differentiation. Proc Natl Acad Sci USA. 2008;105:19762–7.
42. Sasaki T, Hwang H, Nguyen C, Kloner RA, Kahn M. The small molecule Wnt signaling modulator ICG-001 improves contractile function in chronically infarcted rat myocardium. PLoS ONE. 2013;8:e75010.
43. Zhang Z, Deb A, Zhang Z, Pachori A, He W, Guo J, et al. Secreted frizzled related protein 2 protects cells from apoptosis by blocking the effect of canonical Wnt3a. J Mol Cell Cardiol. 2009;46:370–7.
44. Zhou SS, He F, Chen AH, Hao PY, Song XD. Suppression of rat Frizzled-2 attenuates hypoxia/reoxygenation-induced Ca2+accumulation in rat H9c2 cells. Exp Cell Res. 2012;318:1480–91.
45. Tiede I, Fritz G, Strand S, Poppe D, Dvorsky R, Strand D, et al. CD28-dependent Rac1 activation is the molecular target of azathioprine in primary human CD4+T lymphocytes. J Clin Invest. 2003;111:1133–45.
46. Beyersdorf N, Kerkau T, Hunig T. CD28 co-stimulation in T-cell homeostasis: a recent perspective. Immunotargets Ther. 2015;4:111–22.
47. Kallikourdis M, Martini E, Carullo P, Sardi C, Roselli G, Greco CM, et al. T cell costimulation blockade blunts pressure overload-induced heart failure. Nat Commun. 2017;8:14680.
48. Wang H, Kwak D, Fassett J, Hou L, Xu X, Burbach BJ, et al. CD28/B7 deficiency attenuates systolic overload-induced congestive heart failure, myocardial and pulmonary inflammation, and activated T cell accumulation in the heart and lungs. Hypertension . 2016;68:688–96.
49. Reed SG. TGF-beta in infections and infectious diseases. Microbes Infect. 1999;1:1313–25.
50. Dunn KW, Kamocka MM, McDonald JH. A practical guide to evaluating colocalization in biological microscopy. Am J Physiol Cell Physiol. 2011;300:C723–42.